

# The Vector and Scalar Form Factors of the Pion to Two Loops

---

**J. Bijnens**

*Dept. of Theor. Phys. 2, Univ. Lund,  
Sölvegatan 14A, S-22362 Lund, Sweden*

**G. Colangelo**

*INFN–Laboratori Nazionali di Frascati,  
P. O. Box 13, I-00044 Frascati, Italy*

**P. Talavera,**

*Dept. de Física i Enginyeria Nuclear, UPC,  
E-08034 Barcelona, Spain*

**ABSTRACT:** We calculate the vector and scalar form factors of the pion to two loops in Chiral Perturbation Theory. We estimate the unknown  $\mathcal{O}(p^6)$  constants using resonance exchange. We make a careful comparison to the available data and determine two  $\mathcal{O}(p^4)$  constants rather precisely, and two  $\mathcal{O}(p^6)$  constants less precisely. We also use Chiral Perturbation Theory to two loops to extract in a model–independent manner the charge radius of the pion from the available data, and obtain  $\langle r^2 \rangle_V^\pi = 0.437 \pm 0.016 \text{ fm}^2$ .

**KEYWORDS:** Chiral Lagrangians, Spontaneous Symmetry Breaking.

---

## Contents

|  |           |
|--|-----------|
| <b>1. Introduction</b>   | <b>1</b>  |
| <b>2. Definitions and Notation</b>   | <b>4</b>  |
| 2.1 Form factors   | 4         |
| 2.2 Chiral Perturbation Theory   | 4         |
| <b>3. The calculation</b>  | <b>5</b>  |
| 3.1 $F_\pi$ and $M_\pi^2$  | 6         |
| 3.2 Scalar Form Factor   | 7         |
| 3.3 Vector Form Factor   | 8         |
| 3.4 Comparison with earlier work   | 9         |
| <b>4. Resonance and <math>SU(3)</math> estimates of the <math>\mathcal{O}(p^6)</math> parameters</b> | <b>10</b> |
| 4.1 Scalar contributions   | 10        |
| 4.2 Vector contributions   | 11        |
| 4.3 $SU(3)$ contributions  | 12        |
| <b>5. Numerical results and comparison with experiment</b>   | <b>12</b> |
| 5.1 General input parameters   | 12        |
| 5.2 The scalar Form Factor   | 13        |
| 5.2.1 $F_S(0)$ , $F_\pi/F$ and $M_\pi^2/M^2$   | 16        |
| 5.2.2 Modified Omnès representation.   | 17        |
| 5.3 Comparison with data for $F_V$   | 19        |
| 5.3.1 The data and previous analyses   | 19        |
| 5.3.2 Comparison of $\langle r^2 \rangle_V^\pi$ and $c_V^\pi$ with CHPT at two loops                 | 20        |
| 5.3.3 Fit to the data with CHPT at two loops   | 22        |
| 5.3.4 Modified Omnès Representation  | 25        |
| 5.3.5 Hadronic Contribution to the Muon $(g-2)$ and to $\alpha(M_Z^2)$                               | 26        |
| <b>6. Conclusions</b>  | <b>26</b> |

---

## 1. Introduction

Chiral Perturbation Theory (CHPT) [1] is the modern way of exploiting Chiral Symmetry constraints on strongly interacting processes. The mesonic two-flavour sector

was treated in an extensive work to next-to-leading order [2]. The physical processes and amplitudes treated in that reference were  $F_\pi$ ,  $M_\pi^2$ , the scalar and vector form factors of the pion, the pion radiative decay ( $\pi \rightarrow \ell\nu\gamma$ ) and  $\pi\pi$  scattering. Due to recent and planned experimental improvements, more accurate theoretical analyses are needed. The next-to-next-to-leading order of  $F_\pi$ ,  $M_\pi^2$  were calculated in [3, 4], the pion radiative decay in [5] and  $\pi\pi$  scattering in [4, 6]. In addition, the pion polarizabilities and the production of pion pairs in gamma-gamma collisions are also known to this order. For the latter, the neutral process was studied in [7] and the charged case in [3]. In this paper we present the full  $\mathcal{O}(p^6)$  calculation of the scalar and vector pion form factors, thereby completing the calculation to the next order of the processes considered in [2].

In addition to the above calculations there are those where the amplitude is calculated using dispersive methods. This method allows for the full calculation up to the subtraction constants. These have then to be determined by comparison with experiment. The disadvantage of this approach is that one cannot do a simple comparison to existing models of low-energy constants appearing in CHPT, since the “chiral logarithm” parts of the subtraction constants cannot be fully determined<sup>1</sup>. As a consequence, we can neither vary the quark mass to compare with e.g. lattice calculations. The dispersive calculation for the form factors was done in [8], (see [9] for the analogous  $\pi\pi$  calculation) and an analytical expression for the dispersive integrals in the vector form factor was found in [10]. The one-loop formula and the latter partial two-loop results for the vector form factor have been used in the inverse amplitude method to fit over a larger kinematic range [11]. A different resummation scheme using constraints from Vector Meson Dominance (VMD),  $1/N_c$  and unitarity, works as well in extending the range of validity [12]. For a recent review of the form factors in general see Ref. [13].

We have performed the calculation in two different ways. We have used the master formula approach as described in [4] and we have also directly computed all the relevant Feynman diagrams. Several nontrivial checks on the calculation of both form factors were done. The first is the absence of nonlocal divergences, i.e. the dependence on quark masses and external kinematical variables of the divergent parts must be analytic. Another powerful check results from the value of the form factors at zero momentum transfer. For the vector form factor this must be one because of gauge invariance and, for the scalar form factor, it is related to the derivative of the pion mass w.r.t. the quark mass. The latter relation follows from the Feynman–Hellman theorem.

For both form factors we have abundant experimental information to compare with. In the vector case this information consists of direct measurements of the form

---

<sup>1</sup>Sometimes the requirement that the limit  $M_\pi^2 \rightarrow 0$  gives a finite result allows to determine these terms, see [8] for an example.

factor, both in the timelike and spacelike region. In the scalar case, since there is no microscopic scalar probe available, it is impossible to directly measure the form factor. On the other hand, it can be shown that the experimental information on the scalar,  $I = 0 \pi\pi$  phase shifts, inserted in a dispersive representation for the form factor, allows one to completely reconstruct the energy dependence of the form factor, modulo a multiplicative overall factor. Therefore in both cases we can make a detailed comparison of the CHPT two-loop expressions to the available experimental information. The fact that the form factors have a simple kinematical structure, makes even the two-loop representation rather simple and easy to manipulate. For this reason the comparison to the experimental information is particularly instructive.

The contributions at order  $p^6$  can be split into two different pieces: a dispersive contribution and a polynomial part. The numerical contribution of the dispersive part has been already analyzed in Ref. [8]. Inside the polynomial part we have again two types of terms: chiral logarithms and new  $\mathcal{O}(p^6)$  low energy constants (LEC). The splitting between these two types of terms is arbitrary and depends on the renormalization scale  $\mu$ : on the other hand we have learned from the experience at order  $p^4$  that the  $\rho$  mass scale is a sensible choice for understanding the physical origin of these two types of terms. As we will show in our analysis, the same choice seems to be still sensible at order  $p^6$ , since we will be able to understand at least the order of magnitude and sign of the new LEC's with an estimate based on the resonance saturation hypothesis. We will also confirm at order  $p^6$  the Vector Meson Dominance hypothesis, showing the different importance of the resonance contribution in the scalar and in the vector channel. Concerning the vector form factor, we stress that the direct comparison of CHPT to the data allows a reliable, model-independent extraction of the value of the charge radius.

The paper is organized as follows. In Sect. 2 we define the form factors and the notation used. In Sect. 3 we describe the calculation and the checks performed, and give the analytical results for the form-factors and the associated radii. Sect. 4 describes various estimates of the  $\mathcal{O}(p^6)$  constants appearing in the calculation. In Sect. 5 we describe the other numerical input used and fit accurately to the available data for both form factors. Here we also describe the variation of the fits with several different assumptions and provide numerical results for all quantities, including  $F_\pi/F$ ,  $M_\pi^2/M^2$  and an improved estimate of the low energy hadronic vacuum polarization contribution to the muon anomalous magnetic moment. In this section we also discuss the Omnès representation. We finally recapitulate our main conclusions in Sect. 6.

## 2. Definitions and Notation

### 2.1 Form factors

The scalar and vector form factors are defined respectively by

$$\begin{aligned} \langle \pi^i(p_2) | \bar{u}u + \bar{d}d | \pi^j(p_1) \rangle &= \delta^{ij} F_S(s_\pi) , \\ \langle \pi^i(p_2) | \frac{1}{2} (\bar{u}\gamma_\mu u - \bar{d}\gamma_\mu d) | \pi^j(p_1) \rangle &= i\varepsilon^{i3j}(p_{1\mu} + p_{2\mu}) F_V(s_\pi) , \end{aligned} \quad (2.1)$$

where  $s_\pi = (p_2 - p_1)^2$ . The scalar form factor is defined through the isospin-zero scalar source. The isospin-one scalar form factor can be defined analogously but it only starts at  $\mathcal{O}(p^4)$ . The vector form factor is also an isovector, and what we calculate here is its  $I_z = 0$  component. Similar definitions exist for the other isospin components. In what follows we take the isospin limit i.e.  $m_u = m_d = \hat{m}$ , so that the other isospin-one components of the vector form factors are identical to the one we analyze here.

### 2.2 Chiral Perturbation Theory

Quantum chromodynamics with two flavours in the chiral limit has an  $SU(2)_L \times SU(2)_R \equiv O(4)$  symmetry which is spontaneously broken down to  $SU(2)_V \equiv O(3)$ . At low energies, the three resulting Goldstone Bosons are the only relevant degrees of freedom and their interactions are strongly constrained by the underlying symmetry. The three Goldstone Bosons can be identified with the pions and the way of extracting the consequences of the chiral symmetry is Chiral Perturbation Theory. We use the non-linear sigma model or  $O(4)$  parametrization with the external field formalism of Ref. [2].

To lowest order in the low energy expansion,  $\mathcal{O}(p^2)$ , processes are described by the tree-level diagrams of the lagrangian

$$\mathcal{L}_2 = \frac{F^2}{2} \nabla_\mu U^\dagger \nabla_\mu U + F^2 (\chi^T U), \quad (2.2)$$

with the covariant derivative defined by

$$\begin{aligned} \nabla_\mu U^0 &= \partial_\mu U^0 + a_\mu^i(x) U^i, \\ \nabla_\mu U^i &= \partial_\mu U^i + \epsilon^{ikl} v_\mu^k(x) U^l - a_\mu^i(x) U^0, \end{aligned} \quad (2.3)$$

where  $U(x)$  is an  $O(4)$  four-component vector

$$U^T = \left( \sqrt{1 - \frac{\pi^i \pi^i}{F^2}}, \frac{\pi^1}{F}, \frac{\pi^2}{F}, \frac{\pi^3}{F} \right). \quad (2.4)$$

Here  $v^k(x)$  and  $a^i(x)$  are the external vector and axial-vector sources respectively and  $\chi = 2B(s^0, p^i)$  contains the isospin-zero part of the scalar source and the isospin-one part of the pseudoscalar source.

To  $\mathcal{O}(p^4)$  the amplitudes are given by one-loop graphs with vertices from  $\mathcal{L}_2$  and tree-level graphs containing vertices from  $\mathcal{L}_2$  and one vertex from the  $\mathcal{O}(p^4)$  Lagrangian given by

$$\begin{aligned}\mathcal{L}_4 = & l_1(\nabla^\mu U^\dagger \nabla_\mu U)^2 + l_2(\nabla^\mu U^\dagger \nabla^\nu U)(\nabla_\mu U^\dagger \nabla_\nu U) \\ & + l_3(\chi^\dagger U)^2 + l_4(\nabla^\mu \chi^\dagger \nabla_\mu U) + l_5(U^\dagger F^{\mu\nu} F_{\mu\nu} U) \\ & + l_6(\nabla^\mu U^\dagger F_{\mu\nu} \nabla^\nu U) + l_7(\tilde{\chi}^\dagger U)^2 + h_1 \chi^\dagger \chi + h_2 F_{\mu\nu} F^{\mu\nu} \\ & + h_3 \tilde{\chi}^\dagger \tilde{\chi},\end{aligned}\tag{2.5}$$

where the strength tensor  $F_{\mu\nu}$  is defined by

$$(\nabla_\mu \nabla_\nu - \nabla_\nu \nabla_\mu)U = F_{\mu\nu}U,\tag{2.6}$$

and  $\tilde{\chi} = 2B(p^0, s^i)$ .

The  $\mathcal{O}(p^6)$  contributions contain pure two-loop diagrams with vertices from  $\mathcal{L}_2$ , one-loop diagrams with vertices from  $\mathcal{L}_2$  and one vertex from  $\mathcal{L}_4$ , and tree level diagrams with vertices from  $\mathcal{L}_2$  and either two vertices from  $\mathcal{L}_4$  or one vertex from the  $\mathcal{O}(p^6)$  Lagrangian. The latter Lagrangian,  $\mathcal{L}_6$ , can be found in [14].

### 3. The calculation

The calculation has been made using two different methods: in one case, we have calculated directly all the relevant Feynman diagrams with full generality. As an alternative method we use the master equation approach [4], which corresponds to recognizing that a large part of the graphs comes together such that they are one-loop graphs with one of the vertices given either by the one-loop scalar or vector form factor or by the  $\pi\pi$  scattering amplitude with the pion legs off-shell. Some two-loop diagrams with non-overlapping loops have then to be evaluated separately in order to obtain the correct normalization. The integrals have been evaluated using the methods of [15], see also [3, 4, 5]. The subtraction procedure we used is a version of the modified minimal subtraction ( $\overline{\text{MS}}$ ) as described in [4].

Both methods have been used independently and yielded the same result. They also satisfy the requirements of gauge invariance, i.e.  $F_V(0) = 1$ , and of the Feynman–Hellman theorem, i.e.  $F_S(0) = \partial M_\pi^2 / \partial \hat{m}$ . Both constraints couple quite a few diagrams in each process providing thus a good check on the calculations. In addition, at two-loop order there are nonlocal divergences diagram by diagram, which also cancel in the sum. The “double chiral logs” also satisfy the constraints imposed by renormalization, meaning that the terms of the type  $(\log(M_\pi^2/\mu^2))^2$  can always be cast inside the  $k_i$  quantities defined in Sect. 3.1—see [16] for further explanation and references.

### 3.1 $F_\pi$ and $M_\pi^2$

For the sake of completeness we write down here the pion decay constant and the pion mass. This also serves to introduce the notation we use for the other quantities of interest. The difference with the expressions used in [3, 4] is that we have subtracted the infinities using  $\overline{\text{MS}}$  scheme and rewritten the  $\mathcal{O}(p^4)$  part in terms of the physical mass and decay constant of the pion ( $M_\pi^2$  and  $F_\pi$  respectively).

$$\begin{aligned} \frac{F_\pi}{F} = 1 + x_2(l_4^r - L) + x_2^2 \left[ \frac{1}{N} \left( -\frac{1}{2}l_1^r - l_2^r + \frac{29}{12}L \right) - \frac{13}{192} \frac{1}{N^2} \right. \\ \left. + \frac{7}{4}k_1 + k_2 - 2l_3^r l_4^r + 2(l_4^r)^2 - \frac{5}{4}k_4 + r_F^r \right] + \mathcal{O}(x_2^3), \end{aligned} \quad (3.1)$$

and

$$\begin{aligned} \frac{M_\pi^2}{M^2} = 1 + x_2(2l_3^r + \frac{1}{2}L) + x_2^2 \left[ \frac{1}{N} \left( l_1^r + 2l_2^r - \frac{13}{3}L \right) + \frac{163}{96} \frac{1}{N^2} \right. \\ \left. - \frac{7}{2}k_1 - 2k_2 - 4(l_3^r)^2 + 4l_3^r l_4^r - \frac{9}{4}k_3 + \frac{1}{4}k_4 + r_M^r \right] + \mathcal{O}(x_2^3). \end{aligned} \quad (3.2)$$

The constants  $r_F^r$  and  $r_M^r$  denote the contributions from the  $\mathcal{O}(p^6)$  lagrangian after modified minimal subtraction.

We have defined the following quantities

$$\begin{aligned} N &= 16\pi^2, \\ x_2 &= \frac{M_\pi^2}{F_\pi^2}, \\ L &= \frac{1}{N} \log \frac{M_\pi^2}{\mu^2}, \\ k_i &= (4l_i^r - \gamma_i L)L, \\ M^2 &= 2B\hat{m}, \end{aligned} \quad (3.3)$$

$M^2$  being the lowest order pion mass and  $F$  the pion decay constant in the chiral limit. The  $l_i^r$  are the finite part of the coupling constants  $l_i$  in  $\mathcal{L}_4$  after the  $\overline{\text{MS}}$  subtraction, and their values depend on the renormalization scale  $\mu$  as  $\mu^2(d\hat{l}_i^r/d\mu^2) = -(\gamma_i/2N)$ . The  $\gamma_i$  were calculated in [2] and are given by

$$\gamma_1 = \frac{1}{3}; \quad \gamma_2 = \frac{2}{3}; \quad \gamma_3 = -\frac{1}{2}; \quad \gamma_4 = 2; \quad \gamma_5 = -\frac{1}{6}; \quad \gamma_6 = -\frac{1}{3}; \quad \gamma_7 = 0. \quad (3.4)$$

Later we will also follow common use, and discuss the  $\mathcal{O}(p^4)$  LEC's in terms of their scale-invariant combinations, the  $\bar{l}_i$ 's, defined as

$$l_i^r = \frac{\gamma_i}{2N}(\bar{l}_i + NL) . \quad (3.5)$$

### 3.2 Scalar Form Factor

We start with the expression of the scalar form factor to two loops evaluated with the methods described above.

$$F_S(s) = F_S(0) \left\{ 1 + x_2 \left( \frac{1}{2}(2s-1)\bar{J}(s) + s(l_4^r - L - \frac{1}{N}) \right) + x_2^2 \left( P_S^{(2)} + U_S^{(2)} \right) \right\} + \mathcal{O}(x_2^3). \quad (3.6)$$

As has been already mentioned, the two-loop contribution has been split into two parts: the polynomial piece of the amplitude reads

$$\begin{aligned} P_S^{(2)}(s) = & s^2 \left[ -\frac{11}{12}k_1 - \frac{7}{12}k_2 - \frac{1}{4}k_4 \right. \\ & + \frac{1}{N} \left( \frac{7}{1728} - \frac{32}{9}l_1^r - \frac{19}{9}l_2^r - l_4^r + \frac{85}{36}L \right) + \frac{1817}{1296} \frac{1}{N^2} + r_{S3}^r \left. \right] \\ & + s \left[ \frac{31}{6}k_1 + \frac{17}{6}k_2 - k_4 + \frac{1}{N} \left( -\frac{11}{864} + \frac{110}{9}l_1^r + \frac{40}{9}l_2^r - 2l_4^r + \frac{11}{9}L \right) \right. \\ & \left. - \frac{20}{81} \frac{1}{N^2} + 2(l_4^r)^2 - 4l_3^r l_4^r + r_{S2}^r \right], \end{aligned} \quad (3.7)$$

where

$$s = s_\pi/M_\pi^2;$$

while the dispersive piece can be cast in the following form

$$\begin{aligned} U_S^{(2)}(s) = & \bar{J}(s) \left[ \frac{1}{3}l_1^r (11s^2 - 40s + 44) + \frac{1}{3}l_2^r (7s^2 - 20s + 28) \right. \\ & + 5l_3^r + l_4^r \left( s^2 + \frac{3}{2}s - 1 \right) + \frac{1}{18}L \left( -43s^2 + 53s - \frac{119}{2} \right) \\ & \left. + \frac{1}{N} \left( \frac{29}{12}s^2 - \frac{61}{9}s + \frac{391}{36} \right) \right] + \frac{3}{4}K_1(s) + K_2(s) \left( \frac{43}{36}s^2 - \frac{4}{3}s + \frac{1}{4} \right) \\ & + K_3(s) \left( \frac{1}{3}s - \frac{25}{18} \right). \end{aligned} \quad (3.8)$$

The integral functions  $\bar{J}$ ,  $K_1$ ,  $K_2$ ,  $K_3$  and  $K_4$  are defined in [4] and we reproduce them here for the sake of completeness

$$\begin{pmatrix} \bar{J} \\ K_1 \\ K_2 \\ K_3 \end{pmatrix} = \begin{pmatrix} 0 & 0 & z & -4N \\ 0 & z & 0 & 0 \\ 0 & z^2 & 0 & 8 \\ Nz s^{-1} & 0 & \pi^2 (Ns)^{-1} & \pi^2 \end{pmatrix} \begin{pmatrix} h^3 \\ h^2 \\ h \\ -(2N^2)^{-1} \end{pmatrix} \quad (3.9)$$

and

$$K_4 = \frac{1}{sz} \left( \frac{1}{2}K_1 + \frac{1}{3}K_3 + \frac{1}{N}\bar{J} + \frac{(\pi^2 - 6)s}{12N^2} \right), \quad (3.10)$$

where

$$h(s) = \frac{1}{N\sqrt{z}} \ln \frac{\sqrt{z}-1}{\sqrt{z}+1} \quad , \quad z = 1 - \frac{4}{s} . \quad (3.11)$$

The functions  $s^{-1}\bar{J}$  and  $s^{-1}K_i$  are analytic in the complex  $s$ -plane (cut along the positive real axis for  $s \geq 4$ ), and they vanish as  $|s|$  tends to infinity. Their real and imaginary parts are continuous at  $s = 4$ .

We use the form factor at zero momentum transfer given by

$$\begin{aligned} F_S(0) = 2B & \left\{ 1 + x_2 \left( 4l_3^r + L + \frac{1}{2N} \right) \right. \\ & + x_2^2 \left[ \frac{1}{N} \left( -11l_1^r - 2l_2^r - 3l_3^r + l_4^r - \frac{39}{4}L \right) + \frac{97}{96} \frac{1}{N^2} \right. \\ & \left. \left. - 8(l_3^r)^2 + 8l_3^r l_4^r - \frac{21}{2}k_1 - 6k_2 - \frac{21}{4}k_3 + \frac{1}{2}k_4 + r_{S1}^r \right] \right\} + \mathcal{O}(x_2^3) , \end{aligned} \quad (3.12)$$

as a check of the previous result, Eq. (3.6). One can see that this last expression can also be derived using Eq. (3.2) and the Feynman–Hellman theorem. It agrees exactly and leads to the relation between the  $\mathcal{O}(p^6)$  constants  $r_{S1}^r = 3r_M^r$ .

We can now expand the form factor for  $s \ll 1$  ( $s_\pi \ll 4M_\pi^2$ ), obtaining the expression

$$F_S(s) = F_S(0) \left( 1 + \frac{1}{6} \langle r^2 \rangle_S^\pi s + c_S^\pi s^2 + \mathcal{O}(s^3) \right) . \quad (3.13)$$

This serves as the definition of the pion scalar radius  $\langle r^2 \rangle_S^\pi$  and of the coefficient  $c_S^\pi$ . Expanding the integral functions in Eq. (3.6) we obtain

$$\begin{aligned} \langle r^2 \rangle_S^\pi = x_2 & \left( -\frac{13}{2N} + 6l_4^r - 6L \right) \\ & + x_2^2 \left[ \frac{1}{N} \left( -\frac{23}{192} + 88l_1^r + 36l_2^r + 5l_3^r - 13l_4^r + \frac{145}{36}L \right) + \frac{869}{108} \frac{1}{N^2} \right. \\ & \left. - 24l_3^r l_4^r + 12(l_4^r)^2 + 31k_1 + 17k_2 - 6k_4 + 6r_{S2}^r \right] + \mathcal{O}(x_2^3) , \end{aligned} \quad (3.14)$$

and an analogous formula for  $c_S^\pi$

$$\begin{aligned} c_S^\pi = x_2 \frac{1}{N} \frac{19}{120} & + x_2^2 \left[ \frac{1}{N} \left( \frac{5}{1152} - \frac{83}{15}l_1^r - \frac{46}{15}l_2^r + \frac{1}{12}l_3^r - \frac{23}{30}l_4^r + \frac{6041}{2160}L \right) \right. \\ & \left. + \frac{1655}{1296} \frac{1}{N^2} - \frac{11}{12}k_1 - \frac{7}{12}k_2 - \frac{1}{4}k_4 + r_{S3}^r \right] + \mathcal{O}(x_2^3) . \end{aligned} \quad (3.15)$$

### 3.3 Vector Form Factor

As in the previous subsection we start with the general expression for the form factor. In the vector case it is given by

$$F_V = 1 + x_2 \left[ \frac{1}{6} (s-4) \bar{J}(s) + s \left( -l_6^r - \frac{1}{6}L - \frac{1}{18N} \right) \right] + x_2^2 \left( P_V^{(2)} + U_V^{(2)} \right) + \mathcal{O}(x_2^3) . \quad (3.16)$$

One should notice that at zero momentum transfer gauge invariance constrains this form factor to be  $F_V(0) = 1$ .

Once more we find it instructive to split the different contributions to the form factor. The polynomial part of the amplitude is

$$\begin{aligned} P_V^{(2)} = & s^2 \left[ \frac{1}{12} k_1 - \frac{1}{24} k_2 + \frac{1}{24} k_6 \right. \\ & + \frac{1}{9N} \left( l_1^r - \frac{1}{2} l_2^r + \frac{1}{2} l_6^r - \frac{1}{12} L - \frac{1}{384} - \frac{47}{192N} \right) + r_{V2}^r \left. \right] \\ & + s \left[ -\frac{1}{2} k_1 + \frac{1}{4} k_2 - \frac{1}{12} k_4 + \frac{1}{2} k_6 - l_4^r \left( 2l_6^r + \frac{1}{9N} \right) \right. \\ & \left. + \frac{23}{36} \frac{L}{N} + \frac{5}{576N} + \frac{37}{864N^2} + r_{V1}^r \right], \end{aligned} \quad (3.17)$$

and the dispersive part of the form factor is

$$\begin{aligned} U_V^{(2)} = & \bar{J}(s) \left[ \frac{1}{3} l_1^r (-s^2 + 4s) + \frac{1}{6} l_2^r (s^2 - 4s) + \frac{1}{3} l_4^r (s - 4) + \frac{1}{6} l_6^r (-s^2 + 4s) \right. \\ & \left. - \frac{1}{36} L (s^2 + 8s - 48) + \frac{1}{N} \left( \frac{7}{108} s^2 - \frac{97}{108} s + \frac{3}{4} \right) \right] + \frac{1}{9} K_1(s) \\ & + \frac{1}{9} K_2(s) \left( \frac{1}{8} s^2 - s + 4 \right) + \frac{1}{6} K_3(s) \left( s - \frac{1}{3} \right) - \frac{5}{3} K_4(s). \end{aligned} \quad (3.18)$$

We can now expand the form factor for  $s \ll 1$  ( $s_\pi \ll 4M_\pi^2$ ) and obtain the expression

$$F_V = 1 + \frac{1}{6} \langle r^2 \rangle_V^\pi s + c_V^\pi s^2 + \mathcal{O}(s^3), \quad (3.19)$$

where the pion charge radius is then given by

$$\begin{aligned} \langle r^2 \rangle_V^\pi = & x_2 \left( -6l_6^r - L - \frac{1}{N} \right) + x_2^2 \left[ -3k_1 + \frac{3}{2} k_2 - \frac{1}{2} k_4 + 3k_6 - 12l_4^r l_6^r \right. \\ & \left. + \frac{1}{N} \left( -2l_4^r + \frac{31}{6} L + \frac{13}{192} - \frac{181}{48N} \right) + 6r_{V1}^r \right], \end{aligned} \quad (3.20)$$

and

$$\begin{aligned} c_V^\pi = & \frac{x_2}{60N} + x_2^2 \left[ \frac{1}{12} k_1 - \frac{1}{24} k_2 + \frac{1}{24} k_6 + \frac{1}{3N} \left( l_1^r - \frac{1}{2} l_2^r + \frac{1}{10} l_4^r + \frac{1}{2} l_6^r \right) \right. \\ & \left. + \frac{1}{N} \left( -\frac{13}{540} L + \frac{1}{720} - \frac{8429}{25920N} \right) + r_{V2}^r \right]. \end{aligned} \quad (3.21)$$

### 3.4 Comparison with earlier work

In addition to the previously mentioned checks, we can compare to earlier partial results already available in the literature.

For the case of the vector form factor we have checked that the dispersive part agrees up to a polynomial piece with the analytical result for the dispersive part of Ref. [10]. In addition, we have checked that the chiral logarithms that could be obtained from chiral limit arguments agree with those given in Ref. [8].

For the scalar form factor we agree with the earlier result for the pion mass via the Feynman–Hellman theorem for  $F_S(0)$ . We also agree with the chiral logarithms that were obtained in Ref. [8] and, finally we have also checked that our expression for  $F_S(s)$  has the correct absorptive parts as derived in [8].

## 4. Resonance and $SU(3)$ estimates of the $\mathcal{O}(p^6)$ parameters

To estimate higher order corrections due to scalar and vector resonances in both form factors we follow in the remainder Ref. [17], and refer to it for the notation. The  $SU(3)$  contributions come through kaon and eta intermediate states. These estimates are of course scale dependent, resulting therefore in a scale dependent final result. We postpone the scale dependence study to Sect. 5.

The contribution of a given resonance state to  $r_i^r$  is written as  $r_i^R$  with  $R = S, V, K$  (scalars, vectors and kaons respectively), since the effect of higher resonances is expected to be small [17].

In this section, and the for the sake of simplicity, we use a 2 by 2 matrix notation with

$$\begin{aligned} u_\mu &= iu^\dagger \nabla_\mu \overline{U} u^\dagger = u_\mu^\dagger, \\ u^2 &= \overline{U} = U^0 - i\tau^i U^i, \end{aligned} \quad (4.1)$$

the  $\tau^i$  being the Pauli matrices and  $\nabla_\mu$  the relevant covariant derivative as defined in Ref. [17]. We also use

$$\chi_\pm = u^\dagger \chi u^\dagger \pm u \chi^\dagger u, \quad f_{+\mu\nu} = u^\dagger (v_{\mu\nu} + a_{\mu\nu}) u + u (v_{\mu\nu} - a_{\mu\nu}) u^\dagger \quad (4.2)$$

and  $\langle A \rangle = \text{tr}(A)$ .

### 4.1 Scalar contributions

In the scalar form factor the scalar resonance contribution is introduced via the lagrangian

$$\mathcal{L}[S(0^{++})] = \frac{1}{2} \langle \nabla_\mu S \nabla^\mu S - M_S^2 S^2 \rangle + c_d \langle S u_\mu u^\mu \rangle + c_m \langle S \chi_+ \rangle, \quad (4.3)$$

where  $S$  contains the triplet and the singlet scalar in the leading  $1/N_c$  approximation. This corresponds to use  $\tilde{c}_m = c_m/\sqrt{3}$  and  $\tilde{c}_d = c_d/\sqrt{3}$  in the notation of Ref. [17]. We will use the numerical values

$$M_S \approx 980 \text{ MeV}, \quad c_m \approx 42 \text{ MeV} \quad \text{and} \quad c_d \approx 32 \text{ MeV}. \quad (4.4)$$

There are more possible terms than the ones we quote in Eq.(4.3), but there is not enough experimental information on the scalars to determine them. Integrating out the scalars leads to the  $\mathcal{O}(p^6)$  lagrangian

$$\mathcal{L}^S = \frac{-1}{2M_S^4} \left\{ c_m^2 \langle \chi_+ \nabla^2 \chi_+ \rangle + c_d^2 \langle \nabla^2 (u_\alpha u^\alpha) u_\mu u^\mu \rangle + 2c_m c_d \langle u_\mu u^\mu \nabla^2 \chi_+ \rangle \right\}. \quad (4.5)$$

The  $\mathcal{O}(p^4)$  lagrangian also produced in this way is included here via the contributions from  $l_i^r$  terms. There are obviously no contributions to  $r_F^r$ ,  $r_M^r$ ,  $r_{V1}^r$  and  $r_{V2}^r$  from Eq. (4.5). For the rest we obtain (using  $F = F_\pi = 93.2 \text{ MeV}$ )

$$\begin{aligned} r_{S1}^S &= 0, \\ r_{S2}^S &= \frac{4F^2}{M_S^4} c_m (c_m - 2c_d) \approx -0.3 \cdot 10^{-4}, \\ r_{S3}^S &= \frac{4F^2}{M_S^4} c_m c_d \approx 0.5 \cdot 10^{-4}. \end{aligned} \quad (4.6)$$

These results should be taken as nothing more than an order of magnitude estimate for the size of these constants.

## 4.2 Vector contributions

Similarly as was done in [3, 4, 5, 7], we use the formalism where the vector contribution to the chiral Lagrangian starts at  $\mathcal{O}(p^6)$ . The relevant lagrangian reads

$$\mathcal{L}[V(1^{++})] = \frac{-ig_V}{2\sqrt{2}} \langle \hat{V}_{\mu\nu} [u^\mu, u^\nu] \rangle + f_\chi \langle \hat{V}_\mu [u^\mu, \chi_-] \rangle - \frac{f_V}{2\sqrt{2}} \langle \hat{V}_{\mu\nu} f_+^{\mu\nu} \rangle, \quad (4.7)$$

with  $\hat{V}_\mu$  describing the vector meson and  $\hat{V}_{\mu\nu} = \nabla_\mu \hat{V}_\nu - \nabla_\nu \hat{V}_\mu$ . The parameter  $f_V$  can be determined from  $\rho \rightarrow e^+ e^-$  [18] and  $g_V$  and  $f_\chi$  from  $\rho \rightarrow \pi\pi$  and  $K^* \rightarrow K\pi$  [4], (for the latter process we must use the extension to the three-flavour case). This leads to

$$g_V = 0.09, \quad f_\chi = -0.03 \quad \text{and} \quad f_V = 0.20. \quad (4.8)$$

We can now integrate out the vector meson degree of freedom obtaining only a nonvanishing contribution for

$$\begin{aligned} r_{V1}^V &= \frac{2\sqrt{2}f_\chi f_V F^2}{M_V^2} \approx -0.25 \cdot 10^{-3}, \\ r_{V2}^V &= \frac{g_V f_V F^2}{M_V^2} \approx 0.26 \cdot 10^{-3}, \end{aligned} \quad (4.9)$$

where we have used  $M_V = 770 \text{ MeV}$ .

If instead we make use of full VMD in the three-flavour case, the form factor would be described by

$$F_V(q^2) = \frac{M_\rho^2}{M_\rho^2 - q^2} \approx 1 + \frac{q^2}{M_V^2} + \frac{q^4}{M_V^4} - q^2 \frac{(M_\rho^2 - M_V^2)}{M_V^4} + \dots, \quad (4.10)$$

where the last term accounts for isospin-breaking effects. We can now use as a simple estimate<sup>2</sup>  $M_\rho^2 - M_V^2 = (M_{K^*}^2 - M_\rho^2)M_\pi^2/M_K^2$ , leading to very similar numerical values for  $r_{V1}^r$  and  $r_{V2}^r$

$$r_{V1}^r \approx -0.2 \cdot 10^{-3} \quad \text{and} \quad r_{V2}^r \approx 0.21 \cdot 10^{-3}. \quad (4.11)$$

### 4.3 $SU(3)$ contributions

The  $SU(3)$  contributions to the low energy constants  $r_i^r$  come from kaons and etas intermediate states. For the vector form factor we take the expression derived within  $SU(3)$  CHPT [20, 21] and expand it in terms of inverse powers of  $M_K^2$ . This leads to  $r_{V1}^K = 0$  and

$$r_{V2}^K = \frac{F^2}{1920\pi^2 M_K^2} \approx 0.2 \cdot 10^{-5}. \quad (4.12)$$

The result of Eq. (4.12) is trustable but the one for  $r_{V1}^K$  has several additional contributions coming from the relation between  $L_9^r$  and  $l_6^r$ , the chiral logarithms and the relations between  $F_0$  and  $F$  (the decay constant in the chiral limit and in the limit with  $m_u = m_d = 0 \neq m_s$  respectively [22]). We neglect the latter effects since for  $\mu \approx 770$  MeV the derivative of  $M_K^2 \log(M_K^2/\mu^2)$  is very small.

In the scalar form factor case we can similarly expand the expressions of  $SU(3)$  CHPT as given in Ref. [20] and obtain with  $M_K = 495$  MeV

$$\begin{aligned} r_{S1}^K &= 0, \\ r_{S2}^K &= \frac{F^2}{1152\pi^2 M_K^2} \approx 0.3 \cdot 10^{-5}, \\ r_{S3}^K &= \frac{F^2}{384\pi^2 M_K^2} \approx 0.9 \cdot 10^{-5}. \end{aligned} \quad (4.13)$$

$r_{S1}^K$  and  $r_{S2}^K$  get contributions similar to those discussed above and we also neglect them here.  $r_F^K$  and  $r_M^K$  only get contributions of that type, so we set both to zero.

## 5. Numerical results and comparison with experiment

### 5.1 General input parameters

We use as input parameters  $F_\pi = 93.2$  MeV and  $M_\pi = M_{\pi^+} = 139.57$  MeV. We make also use of the more commonly used  $\bar{l}_i$  quantities as defined in Eq. (3.3). We will mainly use the following two sets of values

$$\begin{aligned} \bar{l}_1 &= -1.7, & \bar{l}_2 &= 6.1, & \bar{l}_3 &= 2.9 \quad \text{set I}, \\ \bar{l}_1 &= -1.5, & \bar{l}_2 &= 4.5, & \bar{l}_3 &= 2.9 \quad \text{set II}. \end{aligned} \quad (5.1)$$

---

<sup>2</sup>A more thorough treatment of quark mass corrections as done in [19] for the masses and decay constants would not change any conclusions within the precision needed here.

The value of  $\bar{l}_3$  is in both cases the one derived in [2]. Set I has the other two parameters obtained from the absolute values of the  $K_{l4}$  form factors using a dispersive improved  $\mathcal{O}(p^4)$  CHPT calculation for three flavours [23]. Set II corresponds to using the  $\mathcal{O}(p^6)$  calculation of  $\pi\pi$  scattering and fitting the  $D$ -wave scattering lengths. This set also agrees, within the errors, with other determinations of  $\bar{l}_1$  and  $\bar{l}_2$  from dispersive analyses of  $\pi\pi$  scattering data, see Ref. [24], and Sect. 5.2 of Ref. [4] for a discussion.

In Ref. [2] a value of  $\bar{l}_4 = 4.3$  was also obtained using large  $N_c$  arguments and the measured value of  $F_K/F_\pi$ .

## 5.2 The scalar Form Factor

| $\mu$ (GeV)                            | $\mathcal{O}(p^2)$ | $\mathcal{O}(p^4)$ | $\mathcal{O}(p^6)$ set I |        |        | $\mathcal{O}(p^6)$ set II | $r_i^R$ |
|--|--------------------|--------------------|--------------------------|--------|--------|---------------------------|---------|
|  |                    |                    | 0.5                      | 0.77   | 1.0    |                           |         |
| $\langle r^2 \rangle_S^\pi$ (fm $^2$ ) | 0                  | 0.548              | 0.016                    | 0.017  | 0.025  | 0.054                     | -0.004  |
| $c_S^\pi$ (GeV $^{-4}$ )               | 0                  | 5.93               | 3.41                     | 3.79   | 3.55   | 2.52                      | 0.8     |
| $F_S(0)/(2B)$                          | 1                  | -0.0341            | 0.0081                   | 0.0086 | 0.0080 | 0.0009                    | 0       |
| $F_\pi/F$                              | 1                  | 0.0611             | 0.0061                   | 0.0061 | 0.0063 | 0.0075                    | 0       |
| $M_\pi^2/M^2$                          | 1                  | -0.0206            | 0.0024                   | 0.0026 | 0.0023 | -0.0003                   | 0       |

**Table 1:** Various contributions to the scalar radius  $\langle r^2 \rangle_S^\pi$ ,  $c_S^\pi$ ,  $F_S(0)/(2B)$ ,  $F_\pi/F$  and to  $M_\pi^2/M^2$ . They all use  $\bar{l}_4 = 4.3$ ,  $r_i^r(\mu) = 0$  for the columns labelled  $\mathcal{O}(p^6)$ . The quantities shown here do not depend on  $\bar{l}_{1,2}$  at  $\mathcal{O}(p^4)$ , and therefore are not sensitive to the use of set I or II at this order.

Although the scalar form factor cannot be accessed experimentally, indirect experimental information can be obtained from the data on  $\pi\pi/KK$  scattering using dispersion relations [25]: modulo an overall normalization one can in fact derive the whole energy dependence of the pion scalar form factor, since it goes to zero for  $s \rightarrow \infty$  as can be proven in perturbative QCD. The analysis of [25] can be used to determine rather precise values of  $\langle r^2 \rangle_S^\pi$  and  $c_S^\pi$ . The results for various parametrizations of the relevant phase shifts, labelled by  $A_1$ ,  $A_2$  and  $B$ , give an indication of the uncertainty involved in such quantities. The results are – we refer to [8] for further explanations –

$$\begin{aligned} \langle r^2 \rangle_S^\pi &= 0.57 \text{ fm}^2(A_1) ; \quad 0.61 \text{ fm}^2(A_2) ; \quad 0.60 \text{ fm}^2(B), \\ c_S^\pi &= 10.0 \text{ GeV}^{-4}(A_1) ; 10.9 \text{ GeV}^{-4}(A_2) ; 10.6 \text{ GeV}^{-4}(B). \end{aligned} \quad (5.2)$$

Following [8] we will use B as central value and the range as an indication of the experimental error. The values labelled  $A_1$  and  $A_2$  use the CERN–MUNICH phase shifts [26] and those labelled B the phase shifts of Au et al. [27].

As was already noticed in [8], the one-loop prediction of Gasser and Leutwyler for the scalar radius (using  $\bar{l}_4 = 4.3 \pm 0.9$ ),

$$\langle r^2 \rangle_S^\pi = \frac{x_2}{16\pi^2} \left( 6\bar{l}_4 - \frac{13}{2} \right) + O(x_2^2) = (0.55 \pm 0.15) \text{ fm}^2, \quad (5.3)$$

is in very nice agreement with the dispersive evaluation of Ref. [25]. Using the same value for  $\bar{l}_4$  and set I for the other constants, we can evaluate the corrections to the leading order result in Eq. (5.3) that come from the two-loop calculation (here we use also  $\mu = M_\rho$ , and  $r_{S2}^r(M_\rho) = 0$ )

$$\langle r^2 \rangle_S^\pi = 0.548 + 0.017 = 0.565 \text{ fm}^2. \quad (5.4)$$

These are rather small and go in the right direction to improve the agreement with the experimental information Eq. (5.2). This shows that for this quantity the convergence of the chiral expansion is quite fast, and hence that it can be used reliably to determine rather precisely the constant  $\bar{l}_4$ . The central value  $\langle r^2 \rangle_S^\pi = 0.60 \text{ fm}^2$  given by solution B, is exactly reproduced by  $\bar{l}_4 = 4.47$  (4.29), if we use set I (set II) together with  $\mu = M_\rho$  and  $r_{S2}^r(M_\rho) = 0$ . The influence of the latter constant on the value of  $\bar{l}_4$  is tiny, and can be neglected altogether. There is some dependence on the choice of the scale, as it is illustrated by a variation of  $\mu$  between 1 and 0.5 GeV:  $\bar{l}_4$  varies between 4.43 and 4.47 for set I, and 4.21 and 4.35 for set II. Taking into account the uncertainty in the determination of  $\langle r^2 \rangle_S^\pi$ , and allowing for a range of values between 0.57 and 0.63 fm<sup>2</sup>, we can conclude that

$$\bar{l}_4 = 4.4 \pm 0.3, \quad (5.5)$$

after averaging over what would be obtained with either set I or II (in principle, once the values of  $\bar{l}_{1,2}$  will be better determined, the error on  $\bar{l}_4$  could be reduced even more). We stress that, given the good convergence of the chiral expansion in this case, the effect of yet higher orders (beyond two loops) can be safely neglected.

The value of the coefficient  $c_S^\pi$  at one loop does not depend on low energy constants, but it turns out to be quite far from the experimental number

$$c_S^\pi = \frac{x_2}{16\pi^2} \frac{19}{120} = 5.93 \text{ GeV}^{-4}. \quad (5.6)$$

At two loops the situation improves considerably, although the exact value of this coefficient now depends both on  $\mathcal{O}(p^4)$  and  $\mathcal{O}(p^6)$  low energy constants. Using the value of  $\bar{l}_4$  determined with the scalar radius, we get the following numerical values

$$\begin{aligned} c_S^\pi(\text{set I}) &= 9.85 \text{ GeV}^{-4} + x_2^2 r_{S3}^r(M_\rho), \\ c_S^\pi(\text{set II}) &= 8.59 \text{ GeV}^{-4} + x_2^2 r_{S3}^r(M_\rho). \end{aligned} \quad (5.7)$$

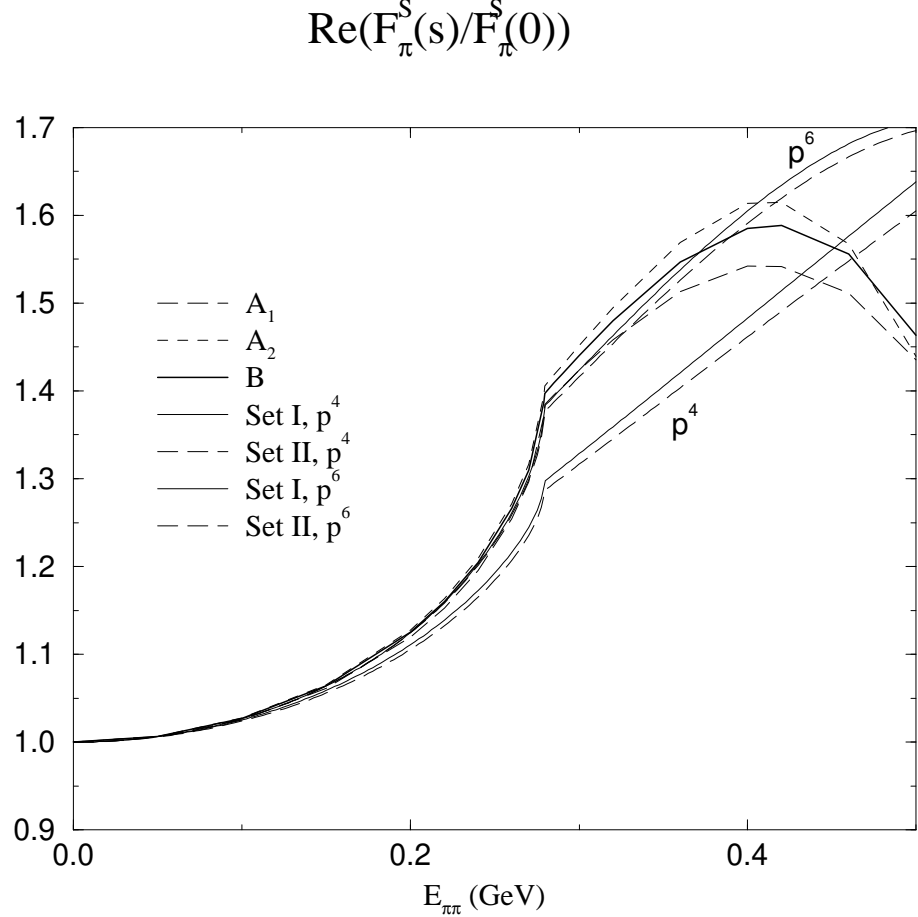


**Figure 1:** The real part of the normalized scalar form factor for the two sets of parameters that reproduce the scalar radius and,  $c_S^\pi$  of set  $B$ , for the two-loop case ( $\mathcal{O}(p^6)$ ) and the one-loop case ( $\mathcal{O}(p^4)$ ).

The two-loop correction to the leading order result is therefore of the right size needed to bring the theoretical number very close to the dispersive determination. To get perfect agreement we could just tune  $r_{S3}^r(M_\rho)$  accordingly, and get  $r_{S3}^r(M_\rho) = 5.6 \times 10^{-5}$  ( $1.5 \times 10^{-4}$ ) for set I (set II). This fine tuning of the  $\mathcal{O}(p^6)$  constant is not especially interesting, were it not for the fact that the value we get is rather close to what we obtained with the resonance saturation hypothesis, Eq. (4.6, 4.13). Notice that the value of  $r_{S3}^r(M_\rho)$  varies by a factor of three when using set I or II, and we should be rather satisfied with an order of magnitude and sign agreement.

If we simply assume naive scalar dominance for the  $l_i^r$  and  $r_i^r$  contributions to the scalar form factor

$$1 + \frac{1}{6} \langle r^2 \rangle_S^\pi s_\pi + c_S^\pi s_\pi^2 \approx \frac{M_S^2}{M_S^2 - s_\pi}, \quad (5.8)$$

we would have obtained  $r_{S3}^r = 8.2 \times 10^{-5}$  and  $l_4^r = 9.0 \times 10^{-3}$  using a value of  $M_S = 980$  MeV. Notice that these values are not so far from the observed ones, being of

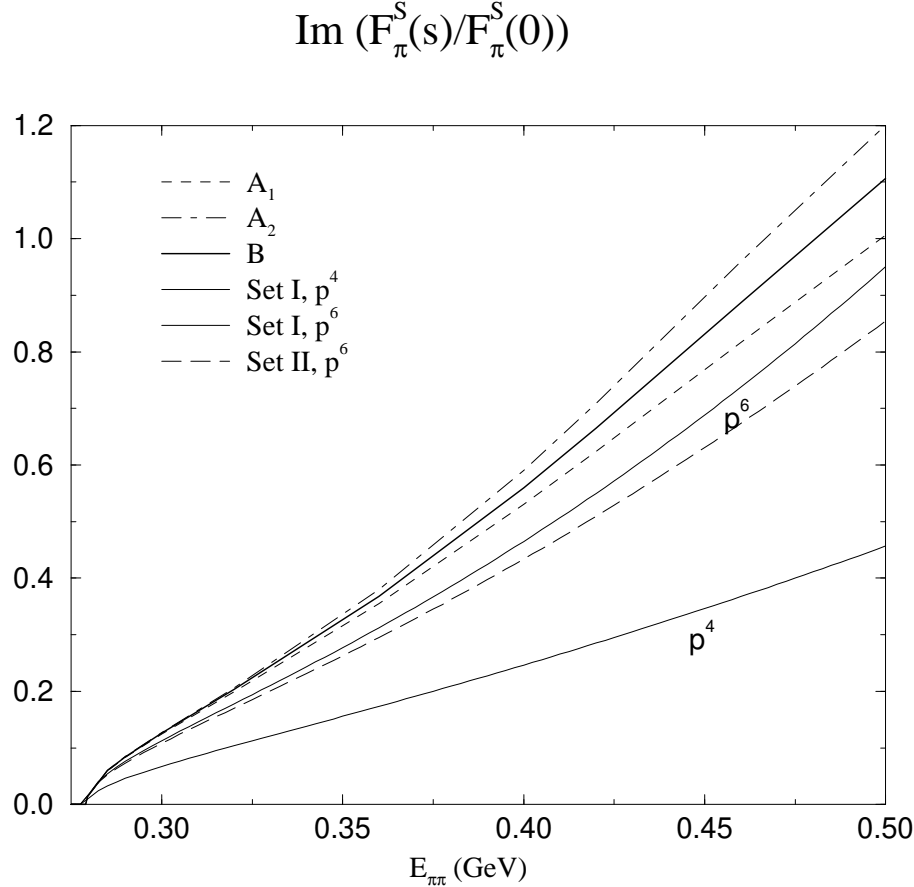


**Figure 2:** The imaginary part of the normalized scalar form factor for the two sets of parameters that reproduce the scalar radius, and  $c_S^\pi$ , of set  $B$  for the two-loop case ( $\mathcal{O}(p^6)$ ) and the one-loop case ( $\mathcal{O}(p^4)$ ), which is identical for both.

the right order of magnitude<sup>3</sup>. A scalar mass of 500 MeV would have increased the values of  $l_4^4$  and  $r_{S3}^r$  by a factor of 3.8 and 15 respectively, bringing them far out of the region determined from experiment.

In Fig. 1 we have shown the real part of the scalar form factor at  $\mathcal{O}(p^4)$  and at  $\mathcal{O}(p^6)$  for set I,  $\mu = 0.77$  GeV,  $\bar{l}_4 = 4.472$ ,  $r_{S2}^r = 0$  and  $r_{S3}^r = 4.9 \cdot 10^{-5}$ , as well as for set II,  $\mu = 0.77$  GeV,  $\bar{l}_4 = 4.29$ ,  $r_{S2}^r = 0$  and  $r_{S3}^r = 16.4 \cdot 10^{-5}$ . In Fig. 2 we have shown the imaginary part for the same approximations, which is of course identical for the two sets at  $\mathcal{O}(p^4)$ .

### 5.2.1 $F_S(0)$ , $F_\pi/F$ and $M_\pi^2/M^2$

In table 1 we also show the various contributions to the value of the scalar form factor at zero momentum transfer compared to its lowest order value. As can be seen, the  $\mathcal{O}(p^6)$  correction is quite small here. For set I,  $\mu = 0.77$  GeV and  $\bar{l}_4 = 4.4$  the value is  $F_S(0)/(2B) = 0.974 + x_2^2 r_{S1}^r$ .  $F_S(0)$  is of course most sensitive to the

<sup>3</sup>A value of  $\bar{l}_4 = 4.4$  corresponds to  $l_4^r = 6.2 \cdot 10^{-3}$  at  $\mu = 0.77$  GeV.

value of  $\bar{l}_3$  on which we have no extra information here. For completeness we have also included in Table 1 the corrections to the ratios  $F_\pi/F$  and  $M_\pi^2/M^2$ . If we use the value  $\bar{l}_4 = 4.4$  calculated assuming the value of  $r_{S2}^r$  derived from scalar exchange we obtain instead

$$\frac{F_\pi}{F} = 1.069 \pm 0.004 \quad \text{and} \quad \frac{M_\pi^2}{M^2} = 0.982. \quad (5.9)$$

The error is determined by looking at the variation in table 1. We do not quote an error on  $M_\pi^2/M^2$  since we have no improved information on  $\bar{l}_3$  here.

### 5.2.2 Modified Omnès representation.

The unitarity condition which must be obeyed by the scalar form factor is satisfied by the following explicit representation, which is due to Omnès:

$$F_S(s) = P(s) e^{\Delta_0(s)}, \quad (5.10)$$

where

$$\Delta_0(s) = \frac{s}{\pi} \int_{4M_\pi^2}^{\infty} \frac{ds'}{s'} \frac{\phi(s')}{s' - s - i\epsilon}, \quad (5.11)$$

and  $P(s)$  is a polynomial which, in the case of the scalar form factor, can be taken to be a constant. In principle, if one would know the phase and inelasticity of  $\pi\pi$  for  $I = 0$ ,  $S$ -wave, one would know also the scalar form factor up to a constant. Since CHPT provides a representation for the phase  $\delta_0^0$ , one could use Eq. (5.10) to exponentiate the result obtained at any given order of the chiral expansion. As discussed in [8], however, there are problems in carrying through this procedure, particularly because of the bad high-energy behaviour of the chiral representation for the phase shifts.

The authors of [8] have instead proposed what they called the “Modified Omnès representation” (MOR), which is defined in the following manner. First they defined the reduced form factor  $\Gamma^\Lambda(s)$ , as

$$\Gamma^{\text{CHPT}} = e^{\Delta_\Lambda(s)} \Gamma^\Lambda(s), \quad (5.12)$$

with

$$\Delta_\Lambda(s) = \frac{s}{\pi} \int_{4M_\pi^2}^{\Lambda^2} \frac{ds'}{s'} \frac{\phi(s')}{s' - s - i\epsilon}. \quad (5.13)$$

The reduced form factor has the following analytic properties:

1. it is analytic in the complex plane, except for a cut along the positive real axis starting at  $s = 16M_\pi^2$ ;
2. it satisfies the dispersion relation

$$\Gamma^\Lambda(s) = 1 + \frac{s}{\pi} \int_{16M_\pi^2}^{\infty} \frac{ds'}{s'} \frac{\text{Im}\Gamma^\Lambda(s')}{s' - s - i\epsilon}; \quad (5.14)$$

3. in the region  $16M_\pi^2 < s < M_K^2$   $\text{Im}\Gamma^\Lambda(s)$  only gets contributions from many particle intermediate states and is hence small.

Given these properties it is easy to show that at low energy  $\Gamma^\Lambda(s)$  can be well approximated by a polynomial. Inserting a polynomial of a given order for  $\Gamma^\Lambda(s)$  on the right-hand side of Eq. (5.12), one obtains the Modified Omnès representation.

Gasser and Meißner have then compared the MOR which they obtained using a linear polynomial for  $\Gamma^\Lambda$  and the phase shift to one loop. Since the CHPT phase is now known to two loops, we can check here what kind of improvements this yields for the MOR. Besides this we also use a quadratic polynomial for  $\Gamma^\Lambda$ , and fix its coefficients such that we reproduce the Taylor expansion at  $s = 0$  as given by the exact solution. The results are shown in Fig. 3, where we compare the MOR with one- or two-loop phase shifts to the exact solution. As can be seen from the figure,

$$\text{Re}(F_\pi^S(s)/F_\pi^S(0))$$

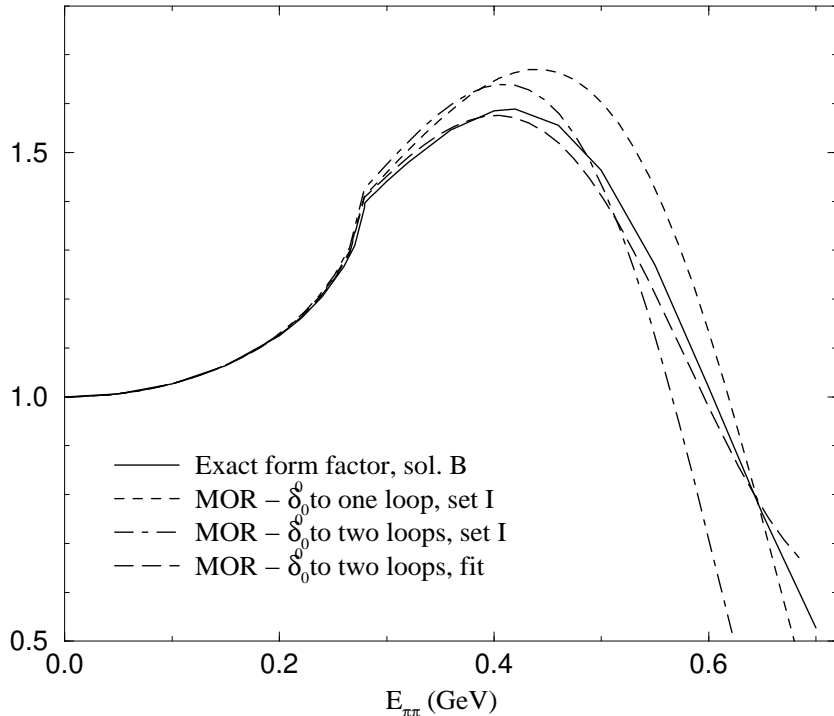


**Figure 3:** Comparison of the Modified Omnès representation (MOR) for the scalar form factor with the exact solution B. For the MOR we have three curves: two are made with set I for the LEC's, and one- or two-loop pion phase shift. The third one (identified by the word “fit”) has been produced with the phase shift at two loops, and by choosing ad hoc values for the constants  $\bar{l}_1 = -1.5$ ,  $\bar{l}_2 = 5.0$ , so as to reproduce as closely as possible the exact solution.

the qualitative features of this representation do not change whether one uses the

one- or two-loop expression for the phase. There is of course a quantitative change which, however, is not very large up to 700 MeV. On this basis one could argue that with this representation and the two-loop phase as input, one can get a rather good description of the form factor up to  $\sim 600$ –700 MeV. The curves relative to set I, that are shown in the figure, seem to contradict this statement as their comparison to the exact form factor is not very good already immediately after threshold. On the other hand the situation improves drastically if we use set II for the LEC's and the two-loop phase. As can be seen from Fig. 3, an impressive agreement up to 700 MeV can be obtained by changing  $\bar{l}_2$  by half a unit with respect to that of set II, i.e.  $\bar{l}_2 = 5.0$ . We do not want to emphasize too much this agreement, since we do not discuss in detail the uncertainties involved. On the other hand we find it interesting that also the scalar form factor analyzed in this manner seems to indicate the need for a lower value of  $\bar{l}_2$  than what was given by the  $K_{l4}$  analysis [23]. In addition, this example just shows very clearly how one can use unitarity to improve the chiral representation, and push it somewhat beyond its typical limits of validity.

### 5.3 Comparison with data for $F_V$

#### 5.3.1 The data and previous analyses

The pion form factor has been measured both in the timelike,  $s > 0$ , and in the spacelike,  $s < 0$ , region. In the spacelike region there are two experiments with a reasonably large data set, Dally et al. [28] and NA7 at CERN [29]. The latter set is an accurate measurement of  $\pi e$  elastic scattering and dominates all fits. It agrees with [28] in the overlap region, where it has significantly smaller errors.

In the timelike region there are more experiments but none of them has a large and accurate data set in the region relevant here. A review of the data before the recent inclusion of  $\tau$ -decays can be found in Ref. [30]. The data are obtained in three ways:  $\tau$ -decays to  $\pi\pi\nu_\tau$  [31],  $e^+e^- \rightarrow \pi^+\pi^-$  in electron positron colliders [30, 32, 33, 34] and  $e^+e^- \rightarrow \pi^+\pi^-$  measured in NA7 [35].

One value of the pion charge radius was obtained in [29] using a pole fit leaving the normalization free, leading to the result<sup>4</sup>

$$\langle r^2 \rangle_V^\pi = 0.431 \pm 0.010 \text{ fm}^2 \quad n = 0.995 \pm 0.002. \quad (5.15)$$

They also used the parametrization of the vector form factor of Ref. [36], which is a Padé approximation to the Omnès formula using the  $\delta_1^1$   $\pi\pi$  phase shift, and obtained

$$\langle r^2 \rangle_V^\pi = 0.439 \pm 0.008 \text{ fm}^2. \quad (5.16)$$

In [21] the same data were fitted to the one-loop CHPT formula obtained in [22] for the three-flavour case. There, the values  $\langle r^2 \rangle_V^\pi = 0.392 \text{ fm}^2$  and  $\langle r^2 \rangle_V^\pi = 0.366 \text{ fm}^2$

---

<sup>4</sup>See below for the definition of  $n$

were obtained from a fit with normalization one and free respectively. The  $\chi^2$  were not as good as for the pole fits and in the latter case the normalization ended up outside the error band given in [29]. The main cause was that the one-loop chiral formula did not satisfactorily describe the higher  $|s|$  data.

In Table 2 we have shown the results of a fit to various sets of data (as specified in the table and explained below in subsection 5.3.3), using Eq. (3.19), and also a pole formula like

$$F_V(s) = \frac{1}{1 - \frac{1}{6}\langle r^2 \rangle_V^\pi s} + \hat{c}_V^\pi s^2. \quad (5.17)$$

Notice that in this case

$$c_V^\pi = \frac{1}{36} \left( \langle r^2 \rangle_V^\pi \right)^2 + \hat{c}_V^\pi. \quad (5.18)$$

Only for the data of [29] we have taken a normalization uncertainty into account. For none of the other experiments is the systematic error even close to the statistical error, with the possible exception of [35]. E.g. the CMD data of [30] have less than a 2% systematic uncertainty at every point. So in all fits below and in the next subsubsection we multiply  $F_V$  by  $n$  for fitting data from [29], and by one for all the other data sets. In the experiment  $n = 1.0000 \pm 0.0045$ .

### 5.3.2 Comparison of $\langle r^2 \rangle_V^\pi$ and $c_V^\pi$ with CHPT at two loops

The charge radius of the pion has been used by Gasser and Leutwyler to determine the low energy constant  $\bar{l}_6$  with the result:  $\bar{l}_6 = 16.5 \pm 0.9$ , that reproduces  $\langle r^2 \rangle_V^\pi = 0.439 \pm 0.03$  fm<sup>2</sup>. Since we do not have other sources of information on  $\bar{l}_6$ , CHPT to two loops can only be used here to refine the determination of this constant. It is instructive to rewrite the two-loop correction in the following form

$$\langle r^2 \rangle_V^\pi = \frac{x_2}{N} \left[ \left( 1 + 2 \frac{x_2}{N} \bar{l}_4 \right) (\tilde{l}_6 - 1) + \frac{x_2}{N} \left( N \frac{13}{192} - \frac{181}{48} \right) \right], \quad (5.19)$$

where we have defined a new constant

$$\tilde{l}_6 = \bar{l}_6 + 6x_2 \left[ N r_{V1}^r + \frac{1}{3} L \left( \frac{19}{12} - \bar{l}_1 + \bar{l}_2 \right) \right], \quad (5.20)$$

which differs from  $\bar{l}_6$  by a scale-independent quantity. From this expression it is clear that (besides the last piece in Eq. (5.19), which is a tiny effect) the two-loop correction to the charge radius consists of two main contributions. Part of the correction is due to the renormalization of  $F \rightarrow F_\pi$  in the leading term, and produces the factor  $1 + 2x_2/N\bar{l}_4$ , which numerically represents a 12% correction. The other part is a pure two-loop effect, and shifts  $\bar{l}_6$  into  $\tilde{l}_6$ . Numerically, this last effect is as follows (using set I)

$$\tilde{l}_6 - \bar{l}_6 = -0.91 + 6N x_2 r_{V1}^r(M_\rho) = -1.44, \quad (5.21)$$

| Param.                       | data set     | $\chi^2/\text{dof}$ | $n$               | $\langle r^2 \rangle_V^\pi \text{ (fm}^2\text{)}$ | $c_V^\pi \text{ (GeV}^{-4}\text{)}$ |
|------------------------------|--------------|---------------------|-------------------|---|-------------------------------------|
| Polynom<br>Eq.(3.19)         | [29]         | 42.4/42             | $0.995 \pm 0.002$ | $0.420 \pm 0.019$                                 | $2.4 \pm 0.5$                       |
|                              | [29] (cut)   | 17.8/22             | $1.000 \pm 0.005$ | $0.478 \pm 0.056$                                 | $5.1 \pm 2.7$                       |
|                              | Spacelike    | 50.5/55             | $0.996 \pm 0.002$ | $0.429 \pm 0.016$                                 | $2.6 \pm 0.4$                       |
|                              | Timelike     | 23.1/20             | irrelevant        | $0.189 \pm 0.098$                                 | $10.6 \pm 2.3$                      |
|                              | All          | 87.7/77             | 0.999             | $0.459 \pm 0.009$                                 | $3.5 \pm 0.2$                       |
| Pole<br>Eq. (5.17)           | [29]         | 41.2/42             | $0.997 \pm 0.003$ | $0.442 \pm 0.022$                                 | $3.85 \pm 0.68$                     |
|                              | [29] (cut)   | 17.7/22             | $1.000 \pm 0.005$ | $0.488 \pm 0.059$                                 | $6.18 \pm 3.1$                      |
|                              | Spacelike    | 48.9/55             | $0.997 \pm 0.002$ | $0.447 \pm 0.018$                                 | $4.0 \pm 0.57$                      |
|                              | Timelike     | 23.2/20             | irrelevant        | $0.191 \pm 0.105$                                 | $10.4 \pm 2.8$                      |
|                              | All          | 76.7/77             | $0.995 \pm 0.002$ | $0.427 \pm 0.007$                                 | $3.36 \pm 0.22$                     |
| CHPT<br>Eq. (3.16)           | [29]         | 41.8/42             | $0.996 \pm 0.002$ | $0.431 \pm 0.019$                                 | $3.20 \pm 0.51$                     |
|                              | [29] (cut)   | 17.8/22             | $1.000 \pm 0.005$ | $0.482 \pm 0.056$                                 | $5.59 \pm 2.8$                      |
|                              | Spacelike    | 49.7/55             | $0.996 \pm 0.002$ | $0.438 \pm 0.016$                                 | $3.35 \pm 0.44$                     |
|                              | Timelike     | 22.9/20             | irrelevant        | $0.134 \pm 0.098$                                 | $11.4 \pm 2.3$                      |
|                              | All          | 84.2/77             | $0.998 \pm 0.002$ | $0.448 \pm 0.009$                                 | $3.68 \pm 0.24$                     |
| Eq. (3.16)<br>$+d_V^\pi s^3$ | All          | 80.7/76             | $0.996 \pm 0.002$ | $0.437 \pm 0.011$                                 | $3.84 \pm 0.25$                     |
|                              | All but [35] | 58.2/72             | $0.997 \pm 0.002$ | $0.453 \pm 0.011$                                 | $4.45 \pm 0.28$                     |

**Table 2:** Various fits to the pion form factor data using the simple parametrizations Eq. (3.19), for the first five rows, the pole formula Eq. (5.17) for the second five rows, and the full two-loop CHPT expression, Eq. (3.16), for the remaining seven. The last two fits include an extra parameter of the form  $d_V^\pi s^3$  added to the two-loop CHPT expression, which the fit determines to be:  $d_V^\pi = 3.0 \pm 1.6 \text{ GeV}^{-6}$  when all data are fitted, and  $d_V^\pi = 4.1 \pm 1.6 \text{ GeV}^{-6}$  when all data but those of Ref. [35] are fitted. In the second of the five data sets used, we applied a cut and used only those data satisfying  $\sqrt{-s} < 300 \text{ MeV}$ . The errors are those that change the  $\chi^2$  by one. All have a free normalization for the data of [29]. See text for details.

where the numerical value after the last equal sign has been obtained inserting for  $r_{V1}^r(M_\rho)$ , our VMD estimate Eq. (4.9). (The use of set II shifts the above values by

+0.17). Modulo the uncertainty coming from the contribution of the  $\mathcal{O}(p^6)$  LEC, this effect is of the order of  $-10\%$ .

The two main effects of the two-loop correction, both around ten percent level, contribute with opposite sign, and tend to cancel each other, resulting in a rather small correction to the radius

$$\begin{aligned}\langle r^2 \rangle_V^\pi(\text{set I}) &= 0.440 + 0.032 + 60.3 \cdot r_{V1}^r(M_\rho) = 0.457 \text{ fm}^2 , \\ \langle r^2 \rangle_V^\pi(\text{set II}) &= 0.440 + 0.037 + 60.3 \cdot r_{V1}^r(M_\rho) = 0.462 \text{ fm}^2 ,\end{aligned}\quad (5.22)$$

where the final value has been obtained using our estimate for the constant  $r_{V1}^r(M_\rho)$ , Eq. (4.9). This result shows that also here, the chiral expansion is converging rapidly, and that the determination of  $\bar{l}_6$  through the charge radius is in principle rather reliable. On the other hand, in this case the new LEC at  $\mathcal{O}(p^6)$  plays a more important role than the corresponding one for the scalar radius case, where the size of the new LEC suggested by resonance saturation gave a negligible contribution. It is clear that lacking an independent source of information on  $r_{V1}^r(M_\rho)$ , we can use the data on the charge radius only to determine the constant  $\bar{l}_6$ . Any attempt to determine only  $\bar{l}_6$  will depend on estimates and/or assumptions on the value of  $r_{V1}^r(M_\rho)$ , at least at the level of a  $\pm 10\%$  uncertainty.

In the case of  $c_V^\pi$ , the contribution of the  $\mathcal{O}(p^6)$  LEC  $r_{V2}^r(M_\rho)$  is even more important

$$c_V^\pi = 0.62 + 1.96 + 1.3 \times 10^4 r_{V2}^r(M_\rho) = 5.4 \text{ GeV}^{-4} , \quad (5.23)$$

where the first factor refers to the one-loop contribution, and the second to the two-loop one with  $r_{V2}^r(M_\rho) = 0$ , evaluated using the old value  $\bar{l}_6 = 16.5$  and set I, and where the final number has been obtained using our VMD estimate Eq. (4.9). The coefficient  $c_V^\pi$  is therefore mainly sensitive to the value of  $r_{V2}^r(M_\rho)$ , and in principle can be used to determine this  $\mathcal{O}(p^6)$  LEC with rather small uncertainties (modulo higher-order contributions).

### 5.3.3 Fit to the data with CHPT at two loops

Besides comparing the vector form factor CHPT formulae with the “experimental values” of the Taylor expansion coefficients at  $s = 0$ , we can attempt a more ambitious use of our two-loop results, and directly fit the data. The reason for this is twofold: first, there are abundant and accurate data precisely in the region of energy where CHPT can be trusted more. Second, in that region, CHPT is certainly less model dependent than other parametrizations used to fit the data (see above), that make various kind of assumptions. The only assumption made in using a CHPT expression is in the truncation of the expansion to a given order – in the present case, the only theoretical bias comes from neglecting contributions of three-loop order in the chiral expansion. As we will see, we can easily estimate such higher order effects and therefore obtain a reliable model-independent value for the two parameters  $\langle r^2 \rangle_V^\pi$  and  $c_V^\pi$ .

Our fit has been made using the expression:

$$F_V(s) = 1 + \frac{1}{6} \langle r^2 \rangle_V^\pi s + c_V^\pi s^2 + f_V(s) + O(s^3) \quad , \quad (5.24)$$

where  $f_V(s)$  can be easily obtained from Eqs. (3.16,3.18). As free parameters in the fit we have used  $\langle r^2 \rangle_V^\pi s$  and  $c_V^\pi$ . It is clear that the advantage of CHPT is that it provides a way to calculate explicitly the function  $f_V(s)$ , whereas in all other cases one can only make guesses about its value. We remark that although the exact numerical value of this function depends on the LEC's, their effect is rather small, and the uncertainty in the knowledge of their value can be neglected altogether. The results of our fits are presented in Table 2, where we have fitted, as before, five different data sets, as specified in the Table. As can be seen there, the results of the CHPT fits are rather close to both those obtained with the simple polynomial parametrization, Eq. (3.19), and to those obtained with the pole formula, Eq. (5.17). This shows that the assumptions made in the two different parametrizations, Eq. (3.19) and Eq. (5.17), are reasonable, and can in fact be partly justified on the basis of CHPT.

To estimate yet higher orders in CHPT we have chosen to introduce an extra term in the polynomial part of Eq. (5.24), of the form  $d_V^\pi s^3$ , and to fit this new parameter from the data. The value we find is  $d_V^\pi = 3.0 \pm 1.6 \text{ GeV}^{-6}$  when we fit all the data, and  $d_V^\pi = 4.1 \pm 1.6 \text{ GeV}^{-6}$  when we fit all the data except those of Ref. [35]. The changes in the values of the charge radius, and of  $c_V^\pi$ , are rather small, as can be seen in Table 2. Moreover, the improvement in the  $\chi^2$  is visible but not dramatic. This shows that there is no need for a large contribution from higher chiral orders, and that we can confidently use this extra parameter  $d_V^\pi$  to estimate their effect. All in all, we conclude that the best values for the charge radius and  $c_V^\pi$  are given by

$$\begin{aligned} \langle r^2 \rangle_V^\pi &= (0.437 \pm 0.016) \text{ fm}^2 , \\ c_V^\pi &= (3.85 \pm 0.60) \text{ GeV}^{-4} , \end{aligned} \quad (5.25)$$

where the error also takes into account the theoretical uncertainty (i.e. we have added in quadrature the statistical error coming from the fit, and the difference in the central values between the fits with and without the cubic term in the polynomial – for the error on  $c_V^\pi$ , however, see below).

In Fig. 4 we have plotted the available experimental data in the spacelike region together with the results of the two fits corresponding to the last two rows of Table 2. The curves corresponding to the same two fits have been plotted in the timelike region, together with the experimental data, in Fig. 5. Notice that the  $\chi^2$  improves significantly if the timelike NA7 data [35] is not considered. Our belief is that in the latter experiment the systematic errors in the timelike region are underestimated. For this reason we have made a fit including all data but those of Ref. [35], to show how much the central values would be shifted. The shift in the charge radius would

still be within the error bars, while that for  $c_V^\pi$  not: in view of this we have enlarged the error bar of this quantity accordingly (see Eq. (5.25)).

### Space like $|F_\pi^V|^2$

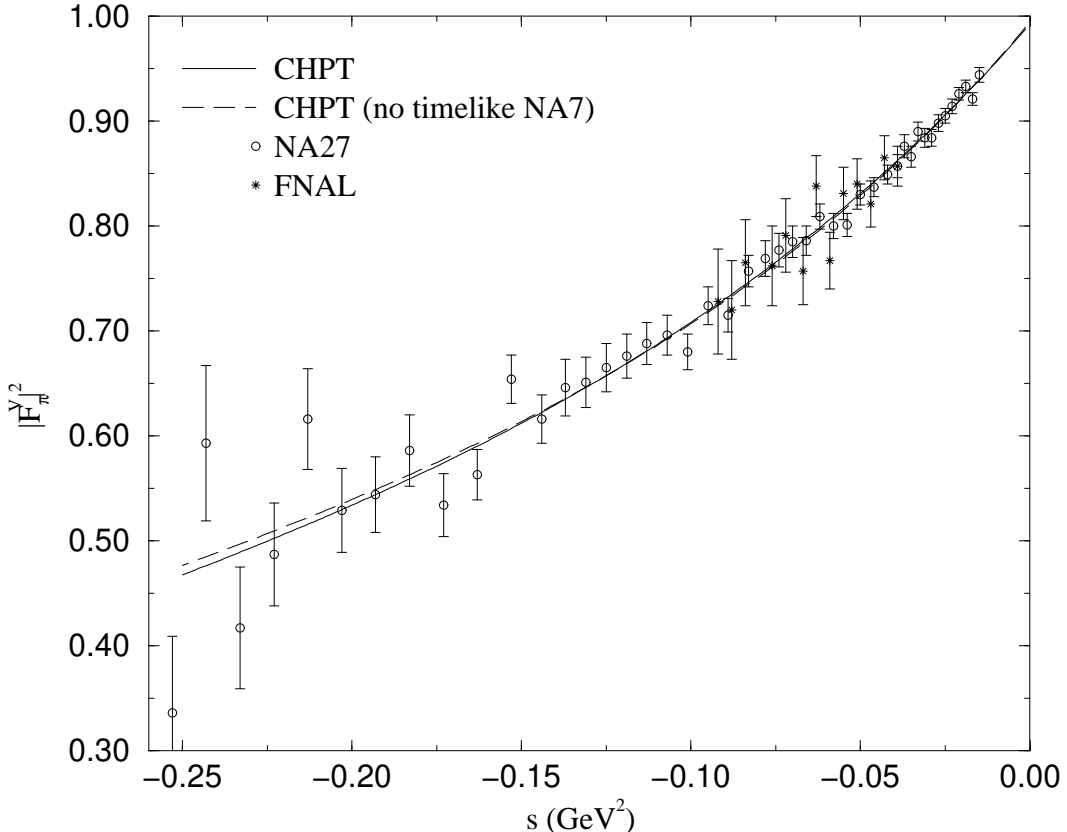


**Figure 4:** The space like data for the vector form factor and the curves corresponding to the fits in the last two rows of Table 2, i.e. using an expression like Eq. (5.24) with the addition of a cubic term in the polynomial.

We can now use the above charge radius and  $c_V^\pi$  determinations to extract the values of the CHPT LEC's  $\bar{l}_6$  and  $r_{V2}^r$ . As we have already stressed, one can unambiguously determine from the charge radius only the constant  $\tilde{l}_6$

$$\tilde{l}_6 = 14.6 \pm 0.5 , \quad (5.26)$$

and if we want to translate this into a value for  $\bar{l}_6$ , we have to make an estimate on the value of  $r_{V1}^r$ . Using our VMD estimate, Eq. (4.9), we get

$$\bar{l}_6 = 16.0 \pm 0.5 \pm 0.7 , \quad (5.27)$$

where the last error is purely theoretical, and takes into account the uncertainty due to the  $r_{V1}^r$  estimate (which we assume to be  $\pm 100\%$ ), and the uncertainty in our

knowledge of  $\bar{l}_{1,2}$ , which also enter  $\tilde{l}_6$ . Compared to the one-loop determination of the same constant, made in [2], we have found a very similar central value (due to the smallness of the two-loop correction we have calculated), but we are able now to make a more reliable error estimate. As we have discussed, there is no way to reduce the error indicated here, which is mainly theoretical. Finally, from the  $c_V^\pi$  value, Eq. (5.25), we get

$$r_{V2}^r(M_\rho) = (1.6 \pm 0.5) \cdot 10^{-4} , \quad (5.28)$$

which is in reasonable agreement with our VMD estimate Eq. (4.9).

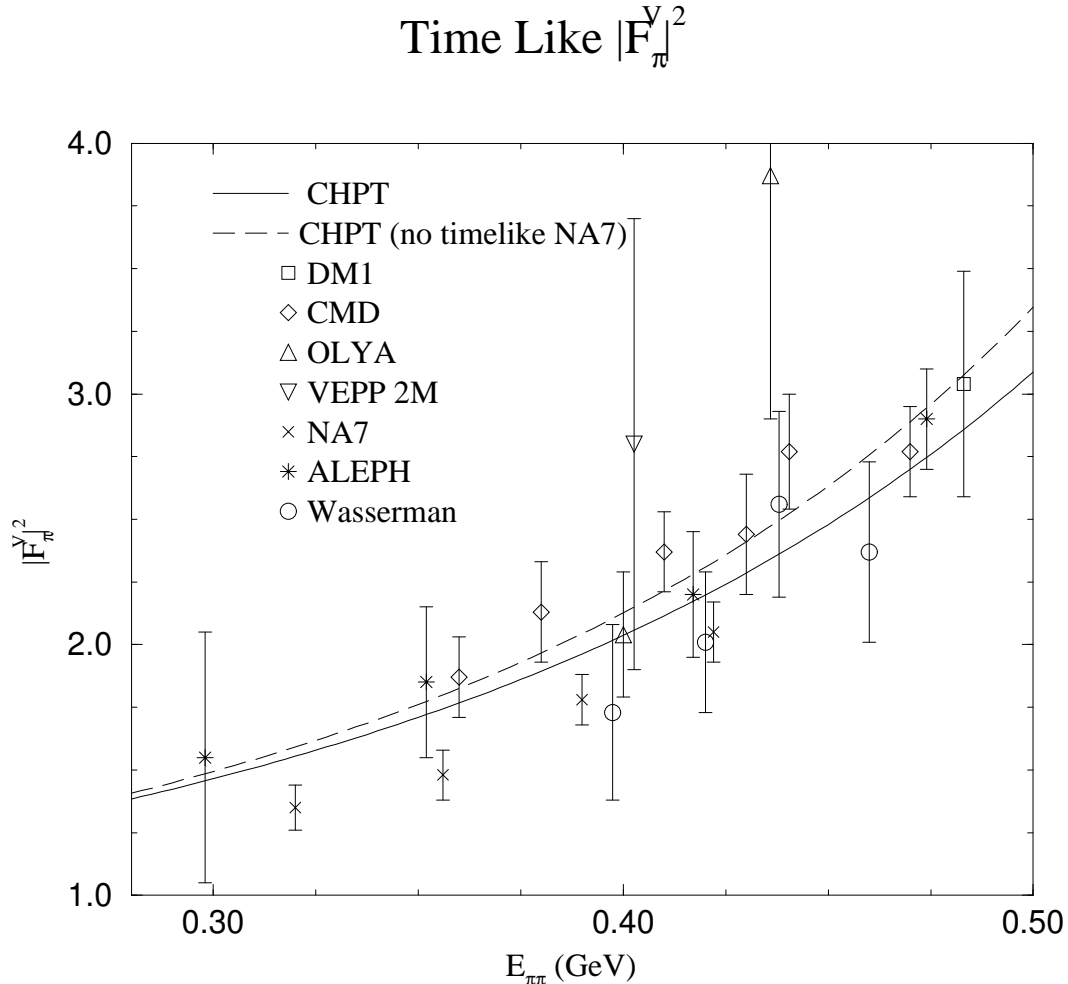


**Figure 5:** The timelike data and two fits as indicated in the caption of Fig. 4.

### 5.3.4 Modified Omnès Representation

In principle we could have tried also for the vector form factor the use of a Modified Omnès Representation, as we did in the scalar case: we could have even used that representation to fit the data. It is clear however that in the vector case the

polynomial part is the largest one, and that exponentiating the small dispersive contribution would not make a big effect. We have actually checked this explicitly and found the effect of the exponentiation to be rather small up to 700 MeV. For this reason we have chosen to estimate the effect of higher orders by including an extra term in the polynomial, as described in the previous subsection.

### 5.3.5 Hadronic Contribution to the Muon $(g - 2)$ and to $\alpha(M_Z^2)$

The process  $e^+e^- \rightarrow \pi^+\pi^-$  is by far the dominant part of the hadronic cross section at low energies. As was shown in the previous subsections, we can get a good fit to the data from Chiral Perturbation Theory up to about 0.5 GeV energies. We can therefore use our results for an improved estimate of the low energy hadronic vacuum-polarization contributions to the muon anomalous magnetic moment and  $\alpha(M_Z^2)$ . For a recent determination and more extensive references see [38]. The relevant formulas are

$$\begin{aligned} a_\mu^{had} &= \frac{\alpha^2(0)}{3\pi^2} \int_{4M_\pi^2}^\infty ds \frac{R(s)K(s)}{s} \\ \Delta\alpha_{had}(M_Z^2) &= -\frac{\alpha M_Z^2}{3\pi} \operatorname{Re} \int_{4M_\pi^2}^\infty ds \frac{R(s)}{s(s - M_Z^2) - i\epsilon}, \\ R(s) &= \frac{3s}{4\pi\alpha^2} \sigma_{\text{tot}}(e^+e^- \rightarrow \text{hadrons}). \end{aligned} \quad (5.29)$$

The function  $K(s)$  is given in [38]. As mentioned above, at low energies we have

$$\sigma(e^+e^- \rightarrow \text{hadrons}) \approx \sigma(e^+e^- \rightarrow \pi^+\pi^-) = \frac{\pi\alpha^2 \left(1 - \frac{4M_\pi^2}{s}\right)^{\frac{3}{2}}}{3s} \left|F_\pi^V(s)\right|^2. \quad (5.30)$$

The total contribution to  $a_\mu^{had}$  is dominated by the  $\rho$  region with a significant fraction from below 500 MeV. The contribution to the various quantities as function of the cutoff  $\Lambda^2$  on the integrals in Eq. (5.29) is given in Table 3 for our result for the CHPT form factor using the fit including all data and the  $d_\pi^V s^3$  term. In brackets we quote the same result but for the fit without the timelike NA7 data. The difference is a reasonable estimate for the error involved. This should be compared to the total results from Ref. [38],  $a_\mu^{had} = (695 \pm 7.5) \cdot 10^{-10}$  and  $\Delta\alpha^{had}(M_Z^2) = (277.8 \pm 2.6) \cdot 10^{-4}$ . From the present analysis the error of  $a_\mu$  coming from the region below 500 MeV is about  $3 \cdot 10^{-10}$ , comparable to the error on the light-by-light scattering contribution [39]. Once the  $\rho$ -mass region is better explored, more work on both the low energy contribution and the light-by-light scattering one will be needed.

## 6. Conclusions

In this paper we have calculated the pion scalar and vector form factor to next-to-next-to-leading order in Chiral Perturbation Theory and presented simple analytical

| $\Lambda$ (GeV) | $10^{10} \cdot a_\mu^{had}$ | $10^4 \cdot \Delta\alpha(M_Z^2)$ |
|-----------------|-----------------------------|----------------------------------|
| 0.32            | 2.38(2.43)                  | 0.039(0.040)                     |
| 0.35            | 7.4(7.6)                    | 0.13(0.14)                       |
| 0.40            | 20.0(20.6)                  | 0.42(0.53)                       |
| 0.45            | 35.7(37.2)                  | 0.86(0.89)                       |
| 0.50            | 53.6(56.3)                  | 1.45(1.53)                       |

**Table 3:** Contributions of the two-pion production to  $a_\mu^{had}$  and  $\Delta\alpha(M_Z^2)$  as a function of the cut-off  $\Lambda$ .

expressions for all the relevant quantities. In addition, we have presented the known formulas for  $F_\pi$  and  $M_\pi^2$  using the same notation.

We have made a careful comparison of these formulas with the data. For the scalar form factor this involves a comparison with the form factor derived using dispersion theory and chiral constraints from the  $\pi\pi$  phase shifts as done in Ref. [25]. The CHPT formula fits well over the entire range of validity. Moreover, we have shown that by using the “modified Omnès representation” as proposed in Ref. [8] and which aims to resum yet higher orders by exponentiating part of the unitarity correction, one can improve the chiral representation, and follow quite closely the exact form factor up to about 700 MeV.

For the vector form factor we have collected all available data of reasonable precision and performed first the standard simple fits to the data sets. Afterwards, we have used the CHPT formula at two loops together with a phenomenological higher order term to obtain a new determination of the pion charge radius and  $c_V^\pi$ :

$$\begin{aligned} \langle r^2 \rangle_V^\pi &= (0.437 \pm 0.016) \text{ fm}^2 , \\ c_V^\pi &= (3.85 \pm 0.60) \text{ GeV}^{-4} . \end{aligned}$$

The error we quote is a combination of theoretical and experimental errors, it covers the variation of the input parameters over the various fits and inputs done using the two-loop CHPT formula.

By comparing the Taylor expansions of the measured form factors, and of their chiral representations, we have been able to better determine some of the LEC’s that appear in these quantities: two of them are the  $\mathcal{O}(p^4)$  constants  $\bar{l}_4$  and  $\bar{l}_6$ , for which we obtained

$$\bar{l}_4 = 4.4 \pm 0.3 \quad \text{and} \quad \bar{l}_6 = 16.0 \pm 0.5 \pm 0.7 , \quad (6.1)$$

where the last error in  $\bar{l}_6$  is purely theoretical, and where we have taken the estimated values of  $r_{V1}^r$  and  $r_{S2}^r$  into account in the values given. Notice that  $\bar{l}_4$  is practically

free from theoretical uncertainties, as we have shown. The new value of  $\bar{l}_6$  together with the  $\mathcal{O}(p^6)$  results quoted in [5] leads to

$$\bar{l}_5 = 13.0 \pm 0.9 . \quad (6.2)$$

The other two LEC's that we have determined are  $\mathcal{O}(p^6)$  constants, that contribute to the quadratic term in the polynomial of the scalar and vector form factors. We found

$$r_{S3}^r(M_\rho) \simeq 1.5 \cdot 10^{-4}, \quad r_{V2}^r(M_\rho) \simeq 1.6 \cdot 10^{-4} , \quad (6.3)$$

with a substantial uncertainty. We find it interesting and encouraging that these values are rather close to the estimates we have made on the basis of the resonance saturation hypothesis. This result gives support to the idea that this hypothesis should work even at order  $p^6$  of the chiral expansion.

## Acknowledgments

We thank R. Urech for permission to include parts of [37], and J. Gasser for enjoyable discussions, and especially for providing us with numerical values of the exact scalar form factor as given in Ref. [8]. PT received support from CICYT research project AEN95-0815. We acknowledge partial support from the EEC-TMR Program, Contract N. CT98-0169.

## References

- [1] J. Bijnens, Int.J.Mod.Phys. A8 (1993) 3045;  
G. Ecker, Prog.Part.Nucl.Phys. 35 (1995) 1;  
H. Leutwyler, *Chiral effective lagrangians*, BUTP-91-26, Lectures given at 30th Int. Universitatswochen fur Kernphysik, Schladming, Austria, Feb. 1991 and at Advanced Theoretical Study Inst. in Elementary Particle Physics, Boulder, CO, June 1991. Published in Boulder TASI 1991 p. 97;  
A. Pich, Rept.Prog.Phys.58 (1995) 563;  
E. de Rafael, Lectures given at Theoretical Advanced Study Institute in Elementary Particle Physics (TASI 94). Published in Boulder TASI 1994 p15.
- [2] J. Gasser and H. Leutwyler, Ann. Phys. 158 (1984) 142
- [3] U. Bürgi, Phys.Lett.B377 (1996) 147; Nucl.Phys.B479 (1996) 392
- [4] J. Bijnens et al., Nucl.Phys. B508 (1997) 263
- [5] J. Bijnens and P. Talavera, Nucl.Phys. B489 (1997) 387.
- [6] J. Bijnens et al., Phys.Lett. B374 (1996) 210.

- [7] S. Bellucci, J. Gasser and M.E. Sainio, Nucl.Phys.B423 (1994) 80, Erratum – ibid. B431 (1994) 413.
- [8] J. Gasser and U.-G. Meißner, Nucl.Phys. B357 (1991) 90.
- [9] M. Knecht et al., Nucl. Phys. B457 (1995) 513.
- [10] G. Colangelo, M. Finkemeier and R. Urech, Phys.Rev. D54 (1996) 4403.
- [11] T. Hannah, Phys.Rev.D54 (1996) 4648
- [12] F. Guerrero and A. Pich, Phys. Lett. B412 (1997) 382;  
F. Guerrero, Phys.Rev. D57 (1998) 4136.
- [13] D. Drechsel et al., *Hadron form factors and polarizabilities, Working Group Summary*, MKPH-T-97-34, nucl-th/9712013.
- [14] H.W. Fearing and S. Scherer, Phys. Rev. **D53** (1996) 315;  
J. Bijnens, G. Colangelo and G. Ecker, work in progress.
- [15] J. Gasser and M. Sainio, *Two Loop Integrals in Chiral Perturbation Theory*, BUTP-98/07, HIP-1998-10/TH, hep-ph/9803251.
- [16] G. Colangelo, Phys.Lett. B350 (1995) 85, Erratum – ibid. B361 (1995) 234.
- [17] G. Ecker et al., Nucl. Phys. B321 (1989) 311.
- [18] G. Ecker et al., Phys. Lett. B223 (1989) 425.
- [19] J. Bijnens, P. Gosdzinsky and P. Talavera, Nucl. Phys. B501 (1997) 495;  
hep-ph/9801418 Phys. Lett. B in press.
- [20] J. Gasser and H. Leutwyler, Nucl. Phys. B250 (1985) 517.
- [21] J. Bijnens and F. Cornet, Nucl. Phys. B296 (1988) 557.
- [22] J. Gasser and H. Leutwyler, Nucl. Phys. B250 (1985) 465.
- [23] J. Bijnens, G. Colangelo and J. Gasser, Nucl. Phys.B427 (1994) 427.
- [24] M. Knecht et al. Nucl. Phys. B471 (1996) 445;  
L. Girlanda et al. Phys. Lett. B409 (1997) 461.
- [25] J. Donoghue, J. Gasser and H. Leutwyler, Nucl. Phys. B343 (1990) 341.
- [26] B. Hyams et al., Nucl. Phys. B64 (1973) 134;  
W. Ochs, Thesis, University of Munich, unpublished
- [27] K.L. Au, D. Morgan and M.R. Pennington, Phys. Rev. D35 (1987) 1633.
- [28] E. Dally et al., (FNAL-E-0216), Phys. Rev. Lett. 48 (1982) 375.
- [29] S. Amendolia et al., (NA7 Coll.), Nucl. Phys. B277 (1986) 168.

- [30] L.M. Barkov et al., (OLYA and CMD coll.), Nucl. Phys. B256 (1985) 365.
- [31] R. Barate et al., (ALEPH coll.), Z.Phys.C76 (1997) 15.
- [32] L.M. Barkov et al., (VEPP 2M), as given in [30].
- [33] A. Quenzer et al., (DM1 Coll.), Phys. Lett. B76 (1978) 512.
- [34] I. Vasserman et al., (TOF coll.), Sov. J. Nucl. Phys. 33 (1981) 709.
- [35] S. Amendolia et al., (NA7 Coll.), Phys. Lett. B138 (1984) 454.
- [36] S. Dubnicka and L. Martinovic, Czech. J. Phys. B29 (1979) 1384.
- [37] G. Colangelo and R. Urech, unpublished.
- [38] R. Alemany et al., Eur. Phys. J. C2 (1998) 123; M. Davier and A. Höcker, [hep-ph/9711308](https://arxiv.org/abs/hep-ph/9711308).
- [39] M. Hayakawa et al., Phys. Rev. D54 (1996) 3137;  
 J. Bijnens et al., Nucl. Phys. B474 (1996) 379. A comparison can be found in J. Bijnens, [hep-ph/9710341](https://arxiv.org/abs/hep-ph/9710341).